The Pennsylvania State University

The Graduate School

College of Engineering

# PERFORMANCE OF STAINLESS STEEL 304 CATHODES AND BICARBONATE BUFFER IN A MICROBIAL ELECTROLYSIS CELL USING A NEW METHOD OF GAS CHARACTERIZATION

A Thesis in

Environmental Engineering

by

Jack R. Ambler



Submitted in Partial Fulfillment
of the Requirements
for the Degree of

Master of Science

August 2010

The thesis of Jack R. Ambler was reviewed and approved* by the following:

Bruce E. Logan
Kappe Professor of Environmental Engineering
Thesis Advisor

John M. Regan
Associate Professor of Environmental Engineering

Peggy Johnson
Professor of Civil Engineering
Head of the Department of Civil and Environmental Engineering

*Signatures are on file in the Graduate School

## ABSTRACT

Microbial electrolysis cells (MECs) have been shown to be efficient devices for the production of hydrogen from organics and inorganics. MECs have been studied extensively that use phosphate buffered solutions and platinum (Pt) cathodes. However, the costs associated with these materials could make scale up expensive and impractical. Several different metal catalysts have been tested in MECs to try to reduce the costs of the cathode, while other buffers have been examined in order to avoid the need for high concentrations of phosphate.

In this study, MECs using a stainless steel 304 (SS304) mesh #60 cathode and a bicarbonate buffer solution were determined to perform comparably to those having a Pt cathode and using a phosphate buffer solution, in terms of hydrogen production per batch cycle, electrical energy efficiency and overall energy efficiency. MEC performance was determined using a new method to evaluate gas production called the gas bag method (GBM). The GBM produced an average error of 5.0 % for known quantities of gasses in the gas bag. The GBM does not require any additional gas flow instruments for gas measurement, which reduces the costs of monitoring MEC performance. Hydrogen production per cycle for 30 mLs of solution at 1 g/L sodium acetate was similar for different MEC conditions, with 26.6 ± 1.8 mL using a SS304 mesh cathode and bicarbonate buffer, 26.4 ± 2.8 mL using a Pt cathode and bicarbonate buffer, and 26.8 ± 2.5 mL with a Pt cathode and phosphate buffer. Electrical energy efficiency was highest with a SS304 cathode and bicarbonate buffer at 159 ± 17 %, when compared to 126 ± 14 % for a Pt cathode and bicarbonate buffer, and 134 ± 17 % for a Pt cathode and phosphate buffer. Maximum hydrogen production rates were lowest with SS304 and bicarbonate at 1.1 ± 0.3 $m^3$ $H_2$-$m^{-3}d^{-1}$, and Pt and bicarbonate at 1.2 ± 0.3 $m^3$ $H_2$-$m^{-3}d^{-1}$, compared to 1.7 ± 0.4 $m^3$ $H_2$-$m^{-3}d^{-1}$ with a Pt cathode and phosphate. Lower hydrogen production rates resulted in increased cycle times, which means a longer time

required for treatment as well as more time for hydrogen loss due to the growth of methanogens. These results show that the GBM can be used to compare performances across different MEC setups and that SS304 mesh cathode with a bicarbonate buffer performs comparably to a platinum cathode with a phosphate buffer.

**TABLE OF CONTENTS**

## LIST OF FIGURES

## LIST OF TABLES

**ACKNOWLEDGEMENTS**

There are many people that I would like to thank for helping me get to this point in my graduate studies at Penn State. First I would like to thank Dr Bruce E. Logan for having me as his student, and for his help and guidance throughout my time here. I would also like to thank Dr Jay Regan and Dr William D. Burgos for being on my thesis committee.

I would like to thank everyone in Dr Logan's research group over the last two years for supporting me in my research. I want to thank David Jones for always being available to offer his technical advice and critical thinking to any of my project plans at any time. I'd like to thank Shaoan Cheng and Doug Call for putting up with my questions when I first arrived here and Roland Cusick for always taking time out of his day to let me bounce ideas off of him. I'd like to thank Geoff Rader and Patrick Kiely for helping review my thesis. I would also like to thank my parents and family for showing support and for helping me get to this point.

The work in this thesis was funded by the King Abdullah University of Science and Technology in Saudi Arabia.

# Chapter 1

## Introduction

Energy is one of the largest issues to face the US going into the future. In 2008 America consumed 99 quadrillion ($10^{15}$) BTUs (quads) [1] and this number is expected to grow to 115 quads by 2035 [2]. Petroleum accounted for 37.3 quads, or 37.5 %, of total energy in 2008 and 26.4 quads, or 94.3 %, of transportation energy [1]. Renewable energy contributed only 7.3 quads (6.4 %) to total energy and 0.9 quads (3.0 %) to transportation energy [1]. Petroleum dependence has created three challenging issues: it is a finite resource; the US does not have the reserves to supply its own demands; and the combustion of petroleum produces large amounts of greenhouse gases.

Petroleum is a non renewable resource for which demand will eventually outpace production. While world wide demand decreased from 2008 to 2009 (86.2 million barrels per day (MBD) to 84.9 MBD), this was likely only due to recent economic instability and possible Chinese demand being underreported [3]. For example for the 2004 to 2007 years demand rose from 82.2 to 86.7 MBD with an average rise of 1.8 % [4, 5]. Petroleum production will not be able to keep up with the increased demand forever. With increased demand the peak oil production capacity is expected to be reached in the next 15 years [6-8]. As oil production peaks other fuel sources will need to be used in concert with oil in order to keep up with the demand in the US.

Petroleum use creates a dependence on outside governments with 74.1 % of the US's annual petroleum consumption being imported in 2008 [1]. Products purchased in the US help keep money in the US economy and move the US to energy independence.

The use of petroleum and other fossil fuels results in green house emissions. In 2008 in the US, petroleum contributed 2.4 billion metric tons carbon dioxide equivalents, or 41.9 % of the

total green house gas emissions from the US [9]. This reliance on liquid fuels in the US will likely drop from 57 % imported liquid fuels in 2008 to 45 % in 2035 [2], with US produced biofuels responsible for most of the decrease in dependence [2].

In order for the US to address the three issues associated with petroleum, a portfolio of options must be considered. With oil production reaching maximum levels and demand continuing to increase, a severe shortage of portable fuels is likely [6]. Hydrogen can be a part of the solution. Hydrogen has the highest energy content per weight compared to other fuels, at 120 MJ/kg, and it can be used in both combustion engines and in fuel cells with the main byproduct being water. However there are no effective stores of hydrogen gas on earth [10], so hydrogen will be used as an energy carrier. $H_2$ can be used as both a portable fuel as well as a method of energy storage.

There are several ways to produce hydrogen sustainably such as biophotolysis, water electrolysis using electricity from a renewable source (e.g., solar or wind), biological water-gas shift reaction, photo-fermentation, and dark fermentation [11]. Biophotolysis is a process that uses algae or other organisms to split $H_2O$ into $H_2$ and $O_2$. Biophotolysis has several technological barriers to overcome such as $O_2$ inhibiting the hydrogenases used in hydrogen evolution, and maximum energy production rates that are no more then 0.38 kJ $L^{-1}hr^{-1}$ [12]. Water electrolysis consists of applying a current to water to split it into $H_2$ and $O_2$. The biological water-gas shift reaction is based on the reaction of carbon monoxide and water to form hydrogen gas and carbon dioxide [11]. Carbon monoxide is needed and methane concentrations in the influent stream need to be kept below 3 % [11]. Photo-fermentation uses microbes' ability to fix nitrogen to produce hydrogen. The nitrogenase enzyme creates hydrogen when fixing $N_2$ gas in nitrogen limiting environments and produces $H_2$ as a byproduct [13]. Significant production of $H_2$ requires modification of the nitrogenase enzyme to allow production to continue with ammonia present and modifications to the hydrogenase enzyme to prevent cells from consuming hydrogen present [13]. The process is energy intensive and requires significant fermentation products as well as

large anaerobic photoreactors [11]. Dark fermentation has high energy flow rates for hydrogen, at ~18 kJ $L^{-1}hr^{-1}$ [14]. Even under ideal circumstances only 33 % of the electrons are recovered as $H_2$, leaving much energy in the form of acids and alcohols [15, 16]. Dark fermentation also requires pretreatment of the media either by heat, BES or sterilization of the influent to prevent methanogen utilization of the hydrogen [15].

In 2005 another method for hydrogen production was invented, in which microbes assisted in the production of hydrogen from a variety of different substrates [16]. The system, an adaption of a microbial fuel cell, was named a microbial electrolysis cell (MEC). In these cells the microbes oxidize organic material at an anode and electrons are sent through a circuit to a cathode, where they combine with protons to form hydrogen. This process does not occur spontaneously so power input is required. The needed voltage applied is less then that needed for water hydrolysis. A minimum theoretical limit of 0.14 V is necessary with acetate as the electron donor as compared to 1.23 V required for water hydrolysis [17-19]. Even with this input energy, the efficiency of the process can have electrical energy efficiencies over 100 % [17, 20-22], where in water electrolysis energy efficiencies are in the range of 56-73 % [19]. This increase in energy efficiency is due to the energy added to the system by the substrate. These systems are envisioned as being used to treat wastewaters and produce hydrogen in a sustainable manner [23].

Most MECs use a platinum catalyst for proton reduction. Platinum is an expensive catalyst, and has been priced at \$39.31 $gram^{-1}$ over the last five years [24]. With 0.5 mg Pt $cm^{-2}$ of cathode, the platinum costs come to \$2,200 $m^{-2}$. There are also significant costs required for a binder for holding the catalyst. Stainless steel and nickel catalysts have been studied as potentially promising low cost replacements to platinum [20, 25, 26].

Buffers are another potential issue in MEC scale up. MEC systems often use a phosphate buffer to create a more favorable solution conductivity which increases hydrogen production [17, 27]. Phosphate can be used to buffer the system to a pH of ~7, and it supplies phosphorus for the organisms to uptake. Phosphate addition to waste streams would be considered a backwards step

in treatment as phosphate is a contaminant found in waste streams which must be treated. Phosphate buffered MECs typically contain phosphate at 1.55 g/L to 6.19 g/L levels [17], and thus this water could not be discharged because of the potential of eutrophication of the receiving bodies of water [28]. The loss of phosphorous for this purpose is also an issue [29].

Bicarbonate has been studied as an alternative buffer in MFCs [30] and MECs [31], and has compared favorably to phosphate buffers. Bicarbonate adds conductivity and can be used to buffer pH changes. Discharging excess bicarbonate to a receiving body could raise the water pH and add alkalinity. The increase in pH caused by the addition of bicarbonate would not need to be adjusted further by expensive bases or acids because MEC systems work most efficiently as the pH of the system approaches the pKa of the buffer [31].

MEC performance is usually evaluated in terms of gas and current production. Gas production is typically measured using gas flow devices, such as respirometers, but these can be expensive and can result in measurement errors [32]. The price of respirometers can also hinder their use in research, as an 8 channel respirometer system typically costs approximately $10,000.

**Research Objectives**

The aim of the research in this thesis was to test the effects that stainless steel 304 cathodes and bicarbonate buffers have on MEC performance using a new gas analysis method. Previous research had shown that a stainless cathode, made in a brush configuration, produced comparable results to a platinum catalyst in a phosphate buffer at an applied voltage of 0.6 V [17, 20]. Bicarbonate buffer has been shown to produce higher power densities than phosphate buffers in a MFC at pH=7 [30]. These previous studies suggested that a stainless steel cathode could be used effectively with a bicarbonate buffer in terms of hydrogen production, and energy efficiency. This combination of buffer and cathode material would be less expensive and therefore more feasible for scaling up MECs. The performance of both Pt and stainless steel cathode materials, in bicarbonate and phosphate buffers, was investigated using a new method of gas characterization

called GBM. The advantage of the GBM method is that it does not require any gas flow measurement devices, and its use can avoid possible gas losses into solution that occur with other gas flow measurement techniques [32].

# Chapter 2

## Literature Review

Hydrogen production from waste biomass is a carbon neutral approach to sustainable energy production. Microbial electrolysis cells (MECs) are a recently discovered process based on microbial fuel cell (MFC) technologies. An MEC works by electrohydrogenesis, where bacteria oxidize the substrate, donate the electrons to the anode and produce protons which go into solution. The electrons travel through the circuit and combine with the protons, usually at a catalytic site, on the cathode and produce hydrogen. The two half reactions for acetate to hydrogen are as follows:

Anode half reaction:

$$CH_3COO^- + 4H_2O \rightarrow 2HCO_3^- + 9H^+ + 8e^- \quad (2.1)$$

Cathode half reaction:

$$8H^+ + 8e^- \rightarrow 4H_2 \quad (2.2)$$

These two reactions at standard biological conditions of temperature, pressure and pH (P=1atm, T=25°C, pH=7) produce this complete reaction and Gibbs' free energy $(\Delta G^{0'})$:

$$CH_3COO^- + 4H_2O \rightarrow 2HCO_3^- + 4H_2 + H^+ \qquad \Delta G_r^{0'} = +104.6kJ \quad (2.3)$$

Since the Gibbs' free energy for this equation is positive the reaction does not occur spontaneously under these conditions, so a power source is used to add energy to the system. A resistor is added to the system to measure voltage drop across the resistor, and current is calculated using Ohm's Law (Figure 2.1).

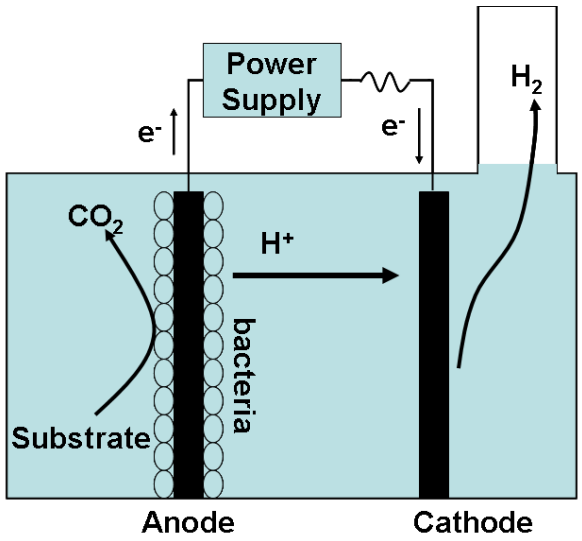


Figure 2.1 Standard single-chamber MEC setup, with the ovals representing microbes. Substrate is oxidized at the anode by the bacteria which produces electrons and protons. Electrons travel through the circuit and combine with the protons at the cathode where $H_2$ is produced [33, 34]

The minimum possible voltage applied to convert a substrate to hydrogen gas can be calculated using the Gibbs free energy, $n$ the number of moles of electrons exchanged in the reaction and $F$ Faraday's constant (96 485 C per mole of electrons) using:

$$E_{ap} = \frac{-\Delta G_r^{0'}}{nF} \tag{2.4}$$

For the reaction in equation 2.3:

$$E_{ap} = -\frac{104.6\ (kJ/mol)}{8\ (mol/eq)\ 96486\ (C/eq)} = -0.14\,V \tag{2.5}$$

This is the minimum voltage addition necessary to produce hydrogen in a MEC reactor fed acetate. In the laboratory hydrogen production has been observed at an applied voltage of 0.2 V [17, 18, 35]. A voltage of 0.2 V is necessary in practice, as opposed to the 0.14 V theoretically needed, because of overpotentials at the anode and cathode and the bacterial energy consumption.

Many MEC reactors contain membranes to separate the anode and cathode [16, 18, 35-38]. The membrane is used to minimize hydrogen transfer to the anode where it could be

consumed. The membrane also separates the gasses produced at the anode from the gasses produced at the cathode, making a purer product gas. A membrane causes a pH gradient across the membrane which can lead to lower pHs at the anode and higher pHs at the cathode, which can cause performance losses [38]. Membranes are expensive and add a significant cost to the MEC system [17, 18, 39]. MEC systems lacking a membrane can produce higher production rates of hydrogen, and similar overall efficiencies to those lacking a membrane [17]. These membrane-less systems produce a mixed product of hydrogen and carbon dioxide which might need to be purified. This presence of $H_2$ in the anode chamber can result in hydrogen losses due to bacterial consumption or to methanogenesis [17, 18, 34].

Many substrates have been tested in MECs, including glucose, cellulose, acetic acid, and lactic acid [37]. Fermentable substrates (glucose and cellulose) produced lower hydrogen recovery, and overall energy efficiencies than non fermentable substrates (acetic acid and lactic acid) in a two chamber system with an anion exchange membrane (AEM) and graphite granule anode [37]. Hydrogen recoveries from fermentable substrates are typically as high as ~70 % while recoveries from non fermentable substrates are 91 % [37]. Overall energy efficiencies have been reported to be ~64 % for fermentable substrates and 82 % for non fermentable substrates [37]. Hydrogen production rates for acetate are reported in the range of 1.02 $m^3$ $H_2$-$m^{-3}d^{-1}$ to 6.32 $m^3$ $H_2$-$m^{-3}d^{-1}$ [17, 40]. For glucose volumetric hydrogen production, values have been reported from 1.23 $m^3$ $H_2$-$m^{-3}d^{-1}$ to 1.87 $m^3$ $H_2$-$m^{-3}d^{-1}$ [22], while cellulose production was at 0.11 $m^3$ $H_2$-$m^{-3}d^{-1}$ [37]. *Geobacter* sp. have been shown to be an important exoelectrogens on MEC anodes [26, 41]. *Geobacter* sp. have a strong affinity to acetate as an electron donor [41]. Lower hydrogen production rates in fermentable substrates could be attributed to the need of the substrate to be broken down to smaller carbon chained molecules to be used by *Gebacter* sp.

Acetate is used as the model substrate in many MEC studies [16, 17, 37, 42]. Acetate can be readily consumed by exoelectrogenic bacteria and is non fermentable. A single chamber membraneless reactor using acetate with a 50 mM phosphate buffer and a platinum catalyst at an

applied voltage of 0.8 V produced 3.12 ± 0.02 $m^3$ $H_2$-$m^{-3}d^{-1}$, with 78 % overall energy efficiency [17]. Electrical efficiency was reported as high as 406 ± 6 % at an applied voltage of 0.3 V, and 194 ± 2 % at an applied voltage 0.8 V [17]. MECs using a stainless steel brush and phosphate buffer at an applied voltage of 0.6 V produced 1.7 ± 0.1 $m^3$-$H_2$ $m^{-3}d^{-1}$, with an electrical energy efficiency of 221 ± 8 % [20].

Several different buffers have been tested in MFCs including bicarbonate, phosphate, MES ($C_6H_{12}NNaO_4S$), HEPES ($C_8H_{18}N_2O_4S$), and PIPES ($C_8H_{18}N_2O_6S_2$) [30, 43], while biotic MECs with a mixed culture have only been tested using a phosphate buffer. Different buffers at similar pHs in abiotic MECs produced similar power densities when their conductivities and pKas are matched [43]. Bicarbonate was not tested in Nam et al's MFC study due to a focus of starting buffer pHs of ~7 [43]. Bicarbonate has a pKa of ~8.76. The use of bicarbonate buffers has been reported in an MEC with active bacteria, but only with pure cultures of bacteria not capable of methane formation [44]. Bicarbonate buffer has been used in a mixed culture and a MEC with a biocathode [42]. Performance with the bicarbonate buffer was not reported, but the author did note that switching to a phosphate based media decreased the loss of hydrogen due to hydrogenotrophic methanogenesis [42]. This was attributed to the lower availability of carbonate for reduction as compared to a phosphate buffer [42]. A 38.6 % higher power density was observed in a bicarbonate buffered MFC at pH 9 than a phosphate buffered MFC at pH 7 when both buffers were at a concentration of 0.2 M [30]. Optimal performance can be expected when the buffer's pH is closest to the buffer's pKa [31]. This is due to the balance of the weak acid catalytic effect and conductivity effect [31]. When the solution pH is near its pKa, some of the weak acids (ex. acetate) are protonated and some are unprotonated. Protonated species are able to donate protons to the catalyst which helps the reaction rate while unprotonated species are charged and contribute to the overall conductivity of the solution [31]. The increase in MFC performance using a bicarbonate buffer compared to a phosphate buffer was attributed to higher diffusion rates of protons carried by bicarbonate compared to monobasic phosphate, and the

smaller sized bicarbonate molecules having more access to smaller catalyst sites [30]. In a separate study comparing bicarbonate and phosphate buffer at pH 7.5 and 100 mM concentration, bicarbonate buffer produced 65.6 % more current density than the phosphate buffer [45]. This was attributed to a higher diffusion coefficient for bicarbonate when compared to phosphate [45]. Conductivities were not reported in this study, and pH was adjusted by the addition of HCl [45]. This addition of HCl to the bicarbonate system to get the pH to 7.5 would have added conductivity, and could have been responsible for the increase of current density.

Stainless steel has been investigated as a possible low price alternative to platinum for an MEC cathode [20, 25, 26]. A stainless steel brush was used to produce hydrogen at rates and efficiencies similar to those achieved with a platinum cathode [20], while in a separate study a sheet of stainless steel compared favorably to a sheet of platinum [25]. SS304 is priced at $3.93/kg [46] as compared to $39 310/kg for platinum [24]. A straight sheet of SS304 has a low actual surface area per projected surface area, meaning few sites are available for the reaction to take place. SS304 brushes can have high specific surface areas, (810 $m^2/m^3$) but bubbles can become trapped in the bristles [20]. These trapped bubbles cause a loss of active surface area as well as an opportunity for biological loss of hydrogen due to hydrogenotrophic methanogenesis [20]. SS304 mesh was investigated as a cathode by Zhang (2010) because mesh can have a high specific surface area (66 $m^2/m^3$). Zhang (2010) showed that SS304 size # 60 was the optimal mesh size compared to several other stainless steel 304 mesh and that bubbles were not observed to stick on the mesh.

The volume of gas produced in an MEC has been measured using several methods including the Owen method [47], bubble displacement in a respirometer [34], and using gas flow devices [42]. In the Owen method, built up gas in the headspace is intermittently released into a gas tight syringe [47]. The pressure in the syringe reaches equilibrium with atmospheric conditions, and after the headspace is sampled the syringe gas is discarded. This approach requires the use of a system capable of withstanding high pressures and it must be gas tight. There

is no additional gas flow equipment required for this method. The build up of pressure due to the product gases can cause an inhibitory effect on hydrogen production in fermentation systems [48].

To get accurate performance data over time, continuous flow monitoring is needed. The use of large amounts of tubing and fittings should be minimized in these system to reduce the loss of gases, especially when low gas production is expected [35]. Hydrogen is the smallest and lightest element, which means it is one of the most difficult to contain within the reactor. The best way to limit $H_2$ loss is to avoid places for the hydrogen to leak from. Continuous gas production has been measured using respirometer systems [17, 25, 37] or flow meters [42]. Gas bags are connected to effluent of these devices to collect gas for characterization with a gas chromatograph. These systems give instantaneous flow data, so production rates can be determined. They are calibrated to a specific gas (usually hydrogen) to be most accurate for that gas type. Errors in these type of measurements are possible and frequent [32]. Biogas can diffuse through the barrier solutions at different rates and cause differences in volumes and compositions [32]. Calibration needs to be done on the low flow gas meters when being used at different flow rates, and corrections for atmospheric conditions should be made in real time [32]. Using a respirometer or a flow meter will give accurate instantaneous gas data but is not exact with the measurement of low flow rate MECs; this combined with a high cost can limit the use of this equipment. The Owen method is a lower cost alternative, however the reactor must be sturdy and air tight and may inhibit biogas production due to the build up of pressure in the system.

# Chapter 3

# Materials and Methods

## 3.1 Materials and Methods

### 3.1.1 Reactor Setup

The MEC reactor body used in experiments was a 4 cm polycarbonate single chamber cubic reactor [17]. The inside was drilled out to produce a cylindrical volume of 28 mL. The anode was an ammonia treated graphite brush (25 mm diameter × 25 mm length; 0.22 $m^2$ surface area; fiber type: PANEX 33 160K, ZOLTEK), with a specific surface area of 18,200 $m^2/m^3$ and a porosity of 95 % [17], placed in the middle of the chamber. All cathodes used were circular with a surface area of 7 $cm^2$. The platinum (Pt) cathodes were wet proofed (30 %) carbon cloth (type B; E-TEK) with 0.5 mg $Pt/cm^2$ and were placed on the side facing the anode (Figure 3.1). The stainless steel cathodes were stainless steel 304 #60 (wire diameter 0.0075 in; pore size 0.009 in.). A section at the top was cut and folded back to allow gas bubbles produced to release freely to the headspace (Figure 3.1). New cathodes were used at the beginning of each set of experiments.

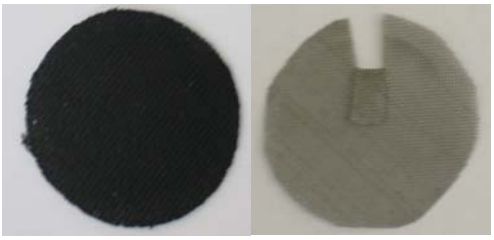

Figure 3.1 A picture of a platinum catalyst (left) and of the SS304 mesh #60 catalyst (right)

Above the cathode, a cylindrical glass tube for gas collection was attached (8 cm length and 1.6 cm diameter) (Figure 3.2). The glass tube was closed by a butyl rubber stopper and an aluminum crimp cap.

Figure 3.2: Picture of a typical MEC cell with brush anode on left and cathode (either platinum or SS304 mesh) on right [49]

### 3.1.2 Start Up and Operation of MEC Cells

The anodes were enriched with electrogenic biofilms by first being run as MFCs [50]. The MFCs were fed with a ratio of 1:1 inoculum and buffered substrate. The inoculum was solution containing suspended bacteria from an MFC which had been operated for more than a year [50]. The substrate buffer solution was 1 g/L sodium acetate in a 50 mM phosphate buffer solution (PBS) ($Na_2HPO_4$ at 4.58 g/L, and $NaH_2PO_4 \cdot H_2O$ at 2.45 g/L along with a nutrient solution of $NH_4Cl$ at 0.31 g/L, KCl at 0.13 g/L) and trace nutrients [50]. The bacterial suspension was no longer added once the MFC voltage reached 0.1 V. Once the MFC reached a stable voltage for three batch cycles then the anode was considered acclimated and used in MECs.

MECs (in duplicate) were fed the same substrate as the MFCs (1 g/L sodium acetate, 50 mM PBS, with trace nutrients and a conductivity of ~7.65 mS/cm) or 80 mM bicarbonate buffer (1 g/L sodium acetate, 6.71 g/L $NaHCO_3$, with $NH_4Cl$ at 0.31g/L, 0.05 g/L $Na_2HPO_4$, 0.03 g/L

$NaH_2PO_4 \bullet H_2O$, and a conductivity of ~7.79 mS/cm; pH was not adjusted). Conductivity and pH of the solution were tested before and after each batch cycle with a VWR Syphony SB21 pH meter and an Oakton Acorn CON 6 conductivity meter. After addition of the medium, the cell was sparged for 20 minutes with ultra high purity (UHP) nitrogen. After each batch cycle the solution was emptied and the reactors were left open to air for ~30 minutes to inhibit growth of methanogens [17]. All batch tests were performed in a temperature controlled room at 30°C. MEC reactors were run for no more than a month before being switched back to MFC mode.

A fixed voltage was applied to the cell using a power source (model 3645A; Circuit Specialists, Inc.). A 10 Ω resistor was connected in series with the power supply and the voltage drop across the resistor was measured using a multimeter (model 2700; Keithley Instruments, Inc.) to determine current. The positive connection of the power source was connected to anode and the negative connection was connected to the resistor and then to the cathode.

### 3.2 Gas Analysis

Gas chromatography was used to analyze the gas in the headspace of the reactor as well as in the gas bags. $H_2$, $N_2$, and $CH_4$ were measured using a gas chromatograph (GC) (SRI Instruments GC 8610B) with an argon carrier and a 6 foot molecular sieve packed 5A column. $CO_2$ was measured using a SRI Instruments GC 310 with a 6 foot porapak Q column. Standards were prepared with pure $H_2$, $N_2$, $CH_4$, and $CO_2$ stocks.

#### 3.2.1 Respirometer Method

Gas volumes and compositions were measured using the respirometer method unless stated. For respirometric tests the MECs were connected to a respirometer (AER-200; Challenge Environmental) and then to a gas bag (0.1 L capacity; Cali-5-Bond, Calibrated Instruments Inc.) (Figure 3.3). Before a gas bag was attached, the gas bag and reactor were sparged with 3 volumes of ultra high purity (UHP) nitrogen (99.998 %) and then the gas bag was emptied using a vacuum

pump. The respirometer operated by counting gas bubbles produced by MEC reactors as they passed through the respirometer cell. The respirometer then recorded the number of bubbles passed and with proper calibration, outputs an instantaneous gas flow rate. After each batch cycle was completed the gas bag and headspace gas composition was analyzed using a gastight syringe (250 μL, Hamilton Samplelock Syringe) using GCs.

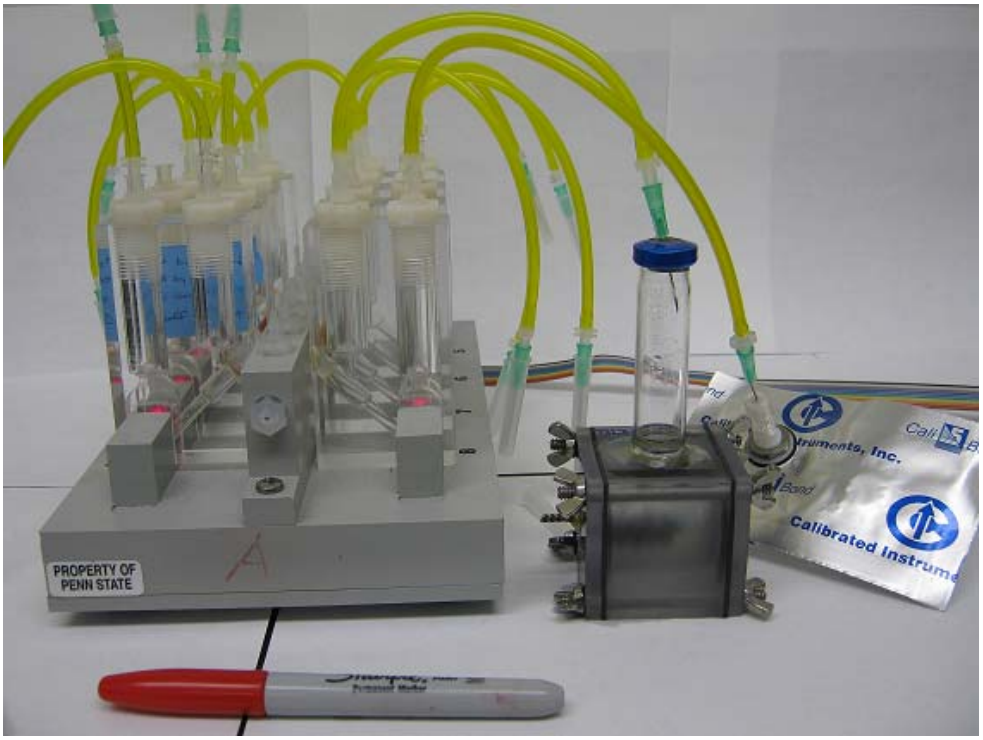


Figure 3.3 Setup for the respirometer method. The cell is attached to a respirometer and then a gas bag.

### 3.2.2 Gas Bag Method

For the GBM the cells were directly connected to a gas bag (Figure 3.4). Before a gas bag was attached, the gas bag and reactor were sparged with 3 volumes of UHP nitrogen (99.998 %). The gas bag was then emptied by applying a vacuum. The MEC was then run for a complete batch cycle. The gas bag and the headspace gasses were then analyzed by using a gastight syringe

(250 µL, Hamilton Samplelock Syringe) by injecting gas samples into the GCs, with the number of injections made recorded. After the gas composition in the gas bag was measured, an additional volume of gas was added to the gas bag using a gas tight syringe (10 mL, Air-Tite Products) to obtain an internal standard. Enough standard gas was added to the system to get an appreciable area change in the GC peaks, which was 10 mL for gas bags containing ~35 - 50 mL. The internal standard in this study was $N_2$ (Appendix D). Other gases that have a good peak response in the GCs and that do not overlap with the measured gases could also be used. After the addition of the internal standard, the gas bag composition was analyzed again using the GC.

Figure 3.4 Setup for the GBM, the cell is attached directly to a gas bag.

### 3.3 Calculations

#### 3.3.1 Respirometer Technique

At the end of each cycle the MEC cells and the gas bags were disconnected from the respirometer and total gas data was recorded from the respirometer. The mole fractions of gases in the headspace and gas bag were calculated based on GC results. Since both the headspace and gas bags were sparged with $N_2$, there was $N_2$ already present in the system that was not produced during MEC operation. Therefore, the mole fractions were calculated on a $N_2$ free basis. The fraction of hydrogen in the gas bag ( $f_{H2,b}$ in $\frac{moles\ H_2}{moles\ H_2 + CO_2 + CH_4}$ ) calculated on a $N_2$ free basis [34]:

$$f_{H2,b} = \frac{x_{H2,b}}{x_{H2,b} + x_{CO2,b} + x_{CH4,b}} \tag{3.1}$$

where the denominator contains the mole fractions in the gas bag, $H_2$ ( $x_{H2,b}$ in $\frac{moles\ H_2}{total\ moles}$ ), $CO_2$ ( $x_{CO2,b}$ ), and $CH_4$ ( $x_{CH4,b}$ ) [34].

The total volume of $H_2$ ( $V_{H2}$ in $mL$ ) can be determined using the total headspace ( $V_h\ mL$ ), the total volume reported by the respirometer ( $V_m$ in $mL$ ), the mole fraction of $H_2$ in the headspace ( $x_{H2,h}$ ), and the amount of nitrogen gas that was displaced from the sparged headspace ( $V_{Hl}\ mL$ ) [34].

$$V_{H2} = x_{H2,h}V_h + f_{H2,b}(V_m - V_{hl}) \tag{3.2}$$

Nitrogen loss from the headspace to the gas bag was found from the percentage of nitrogen in the headspace ( $x_{N,h}$ ) [34].

$$V_{hl} = (1 - x_{N,h})V_h \tag{3.3}$$

Equations 3.1 and 3.2 can be repeated to determine the volumes of $CO_2$ and $CH_4$ by replacing the variables/values for $H_2$ with the variables/values of the gas of interest.

For example the total $CO_2$ can be calculated by:

$$V_{CO2} = x_{CO2,h}V_h + f_{CO2,b}(V_m - V_{hl})$$

### 3.3.2 Gas Bag Method

After a batch cycle was complete the MEC was disconnected from the gas bag, and the gas bag and MEC headspace were analyzed using a GC. A known amount of tracer gas was then added to the gas bag and the gas bag composition was analyzed again. The increase in the mole fraction of the tracer gas due to the tracer addition was used to determine the total volume of gas in the gas bag. The exact values can be calculated using the following equations.

The number of GC injections done on the gas bag before the addition of the tracer gas, ($i$), and the volume of the syringe, ($V_S$ in $mL$), are used to correct for total volume lost ($V_L$ in $mL$) during injections:

$$V_L = i\ V_S \tag{3.4}$$

The initial volume of tracer gas in the gas bag before addition of the tracer gas, ($V_{T,b,i}$ in $mL$), is based on the initial tracer gas mole percentage in the gas bag ($x_{T,b,i}$) and total volume in the bag initial ($V_{b,i}$):

$$V_{T,b,i} = x_{T,b,i}\ V_{b,i} \tag{3.5}$$

The amount of standard gas added ($V_{T,b,a}$) is known. The equation for the mole percentage of tracer in the gas bag after the addition ($x_{T,b,f}$) is:

$$\frac{V_{T,b,i} + V_{T,b,a} - V_L \dfrac{V_{T,b,i}}{V_{b,i}}}{V_{b,i} + V_{T,b,a} - V_L} = x_{T,b,f} \tag{3.6}$$

Combining this with the initial mole percentage of tracer gas in the gas bag solves for the volume in the gas bag initially:

$$V_{b,i} = \frac{-V_{T,b,a} + V_L x_{T,b,i} + V_{T,b,a} x_{T,b,f} - V_L x_{T,b,f}}{x_{T,b,i} - x_{T,b,f}} \quad (3.7)$$

The total volume of hydrogen can be determined using the initial mole percentage of hydrogen in the gas bag ( $x_{H2,b,i}$ ) as well as the headspace hydrogen percentages and the volume of the headspace:

$$V_{H2} = x_{H2,h} V_h + x_{H2,b,i} V_{b,i} \quad (3.8)$$

It can also be calculated using the final percentage of hydrogen in the gas bag ( $x_{H2,b,f}$ ):

$$V_{H2} = x_{H2,h} V_h + x_{H2,b,f} (V_{b,i} + V_{T,b,a}) \quad (3.9)$$

These calculations can be repeated for any of the gases of interest, with the replacement of hydrogen values/variables with those for another gas. An example for testing a gas bag can be seen in Appendix A.

In order to determine if the GBM was viable for measuring gas production and composition, experiments with known amounts of gases were performed. A gas bag was sparged with UHP $N_2$ gas for 3+ pore volumes (15-20 minutes) and then all gas was removed by suction using a vacuum pump. Quantities of $H_2$, $CO_2$, $N_2$ and $CH_4$ similar to volumes found in a typical MEC gas bag were then added to gas bags using a gas tight syringe (10 mL, Air-Tite Products). The procedure outlined was run using triplicate bags and triplicate injections into the GC. Error in calculated $N_2$ values were not reported due to residual $N_2$ left in the bag from the sparging process.

To identify possible losses of biogas, a standard MEC cell was run while connected to the respirometer system. The respirometer was sparged with $N_2$ before each cycle (with ~60 mL) to remove all other gasses. The cell was then run for a complete cycle. Then, 40 mLs of Ar (~2 or 3 volumes) were injected into the system to push any remaining biogas in the headspace of the respirometer or the tubes into the gas bag for collection. Gas production was characterized using the respirometer method, and then checked with the GBM.

### 3.3.3 Hydrogen Yield Calculations

All energy calculations were done as described in Call et al. [17] and Logan [18, 34], as summarized below. Reactor performance was examined in terms of hydrogen recovery, energy recovery, volumetric density, and hydrogen production rate. The theoretical number of moles produced based on substrate usage ( $n_{th}$ ) was calculated with:

$$n_{th} = \frac{b_{H2/s} v_L \Delta S}{M_S} \tag{3.10}$$

where the maximum stoichiometric production of hydrogen based on the substrate ( $b_{H2/S}$ ) is 4 mole/mol acetate; the liquid volume of the reactor ( $v_L$ ) is 30 mL; the change in substrate concentration over the batch period ( $\Delta S$ ) is 0.72 g/L; and the molecular weight of the substrate ( $M_S$ ) is 58.08 g/mole.

The maximum number of moles of hydrogen that could be recovered based on the current values ( $n_{CE}$ ) was calculated by:

$$n_{CD} = \frac{\int_{t=0}^{t} I dt}{2F} \tag{3.11}$$

where $F$ is Faraday's constant (96 485 C/mol electron), $dt$ is the voltage recording interval (20 minutes), and 2 is the ratio of moles of electrons per mole of $H_2$.

The current across the resistor ( $I$ ) was calculated from the output voltage readings using $I = V / R_{ex}$,

The coulombic hydrogen recovery ( $r_{CDE}$ ) is the same as the coulombic efficiency ( $C_E$ ) (the numbers of electrons recovered in the system over the number of electrons theoretically available from the substrate), and is calculated by:

$$r_{CE} = \frac{n_{CE}}{n_{th}} = C_E \tag{3.12}$$

The cathodic hydrogen recovery ( $r_{Cat}$ ) was calculated by:

$$r_{Cat} = \frac{n_{H2}}{n_{CE}} \tag{3.13}$$

where $r_{Cat}$ is the number of moles of hydrogen recovered during the batch cycle ( $n_{H2}$ ) divided by the possible number of moles of hydrogen available based on current ( $n_{CE}$ ).

The maximum volumetric hydrogen production was calculated by:

$$Q_{H2} = 3.68 \times 10^{-5} I_V T r_{Cat} \tag{3.14}$$

where ( $I_V$ ) is the volumetric current density, ( $T$ ), the temperature in Kelvin and $r_{Cat}$, the cathodic hydrogen recovery. The current density is averaged over four hours of maximum current production for a batch cycle. The volume $3.68*10^{-5}$ is the constant that includes faraday's constant, 1 atm of pressure and unit conversions.

### 3.3.4 Energy Calculations

Energy added to the circuit by the applied voltage ( $W_E$ ), with adjustments made for losses across the resistor is calculated by:

$$W_E = \sum_{1}^{n} (IE_{ap}\Delta t - I^2 R_{ex}\Delta t) \tag{3.15}$$

where the current across the resistor ( $I$ ), the applied voltage from the power source ( $E_{ap}$ ), the time change between data points ( $\Delta t$ ) for the number of data points ( $n$ ), and the external resistance ( $R_{ex}$ ).

The work added to the system by the substrate ($W_S$) is calculated by:

$$W_S = -\Delta H_S \, n_S \tag{3.16}$$

with the heat of combustion of the substrate ($\Delta H_S$), (870.28 kJ/mol acetate [18]), and the number of moles of substrate consumed during the batch cycle ($n_S$).

Energy recovered from the system as hydrogen ($W_{H2}$) is calculated by:

$$W_{H2} = \Delta H_{H2} \, n_{H2} \tag{3.17}$$

with the heat of combustion of hydrogen ($\Delta H_{H2}$), (285.83 kJ/mol $H_2$ [18]), and the number of moles of hydrogen recovered ($n_{H2}$).

Energy efficiency based on the energy added to the circuit ($\eta_E$) is calculated by:

$$\eta_E = \frac{W_{H2}}{W_E} \tag{3.18}$$

This term compares the energy recovered as hydrogen to the energy added by the applied voltage.

Energy efficiency taking into account the energy provided by the substrate ($\eta_{E+S}$) is determined by:

$$\eta_{E+S} = \frac{W_{H2}}{W_E + W_S} \tag{3.19}$$

This term compares the energy recovered as hydrogen to the energy added by both the substrate and applied voltage.

# Chapter 4

## Results

### 4.1 Gas Bag Method Proof

The maximum error using the GBM was 5.8 % when comparing measured additions of gases to the calculated results (Table 4.1). $CH_4$ error was the greatest at 5.8 %, with $H_2$ at 5.6 % and $CO_2$ at 3.6 % (Table 4.1).

Table 4.1: Comparison of known additions of $H_2$, $CO_2$ and $CH_4$ to calculated values using GBM (n=4)

| Constituents | mLs Gas Added | GBM Calculated Results | Percent Error |
|---|---|---|---|
| $N_2$* | 10 ± 0.2 | 11.4 ± 1.4 | |
| $H_2$ | 20 ± 0.4 | 21.1 ± 1.1 | 5.6 % |
| $CO_2$ | 5 ± 0.2 | 4.8 ± 0.4 | 3.6 % |
| $CH_4$ | 5 ± 0.2 | 5.3 ± 0.2 | 5.8 % |

*$N_2$ results are expected to be higher than $N_2$ added due to residual gas left over from sparging

### 4.2 Gas Bag Check of Respirometer Method Gas Volume Results

$H_2$ gas production calculated using the respirometer method were 27.6 ± 1.2 mL $H_2$, using the GBM, hydrogen production was only 23.2 ± 3.2 mL $H_2$ (Table 4.2). Total gas produced was calculated at 30.2 ± 1.5 mL $H_2$ with the respirometer and 25.4 ± 3.5 mL $H_2$ using the GBM on the system (Table 4.2). The percentage of hydrogen gas in the system was similar using the two methods at 91.4 ± 0.01 for the respirometer, and 91.1 ± 0.01 for the gas bag (Table 4.2)

Table 4.2: Hydrogen and total gas recoveries from several cell cycles attached to a respirometer, GBM was used after the runs to compare gas recovery (n=7)

| Method | $H_2$ Produced (mL) | Total Gas (mL) | Percent $H_2$ (%) |
|---|---|---|---|
| Respirometer | 27.6 ± 1.2 | 30.2 ± 1.5 | 91.4 ± 0.01 |
| Gas Bag | 23.2 ± 3.2 | 25.4 ± 3.5 | 91.1 ± 0.01 |

**4.3 pH and Conductivity**

Initial conductivity of the bicarbonate and phosphate buffers with 1 g/L sodium acetate were comparable at 7.79 ± 0.07 mS $cm^{-1}$ and 7.65 ± 0.07 mS $cm^{-1}$ respectively (Table 4.3). The change in conductivity during the batch cycle was negligible with no change greater then 0.13 mS $cm^{-1}$ or 1.67 % (Table 4.3). The initial pH of the bicarbonate buffer was 8.94 ± 0.23, while the initial pH of the phosphate buffer was 7.14 ± 0.02. The pH did not change appreciably during the batch cycle with the maximum shift being 0.2 pH units in the bicarbonate buffer (Table 4.3).

Table 4.3: Conductivity and pH data for 3 cell types before and after each batch cycle

| Cell Setup | Media Conductivity Initial (mS/cm) | Media Conductivity Final (mS/cm) | Media pH Initial | Media pH Final |
|---|---|---|---|---|
| Bicarbonate buffer + SS304 Mesh Cathode | 7.79 ± 0.07 | 7.92  0.12 | 8.94 ± 0.23 | 8.98 ± 0.08 |
| Bicarbonate buffer + Platinum Cathode | 7.79 ± 0.07 | 7.86 ± 0.10 | 8.94 ± 0.23 | 9.04 ± 0.17 |
| Phosphate Buffer + Platinum Cathode | 7.65 ± 0.07 | 7.69 ± 0.07 | 7.08 ± 0.02 | 7.14 ± 0.10 |

**4.4 Hydrogen Production Extent**

Hydrogen production was similar when compared across setups. MEC tests with the respirometer method (Resp) at 0.9 V applied voltage produced 29.8 ± 3.4 mL $H_2$ using a platinum cathode with phosphate buffer, 28.8 ± 3.5 mL $H_2$ using a platinum cathode with bicarbonate buffer, and 30.9 ± 1.4 mL $H_2$ using a SS304 #60 mesh cathode and bicarbonate buffer (Figure 4.1). Separate tests done with the GBM produced lower results of 26.8 ± 2.5 mL $H_2$ using a

platinum cathode with phosphate buffer, 26.4 ± 2.8 mL $H_2$ using a platinum cathode with bicarbonate buffer and 26.6 ± 1.8 mL $H_2$ using a SS304 #60 mesh cathode with bicarbonate buffer (Figure 4.1). Methane production was always $\leq$ 0.2 mL for all reactors. Lower $H_2$ volumes measured with the GBM were consistent with the standard addition experiments.

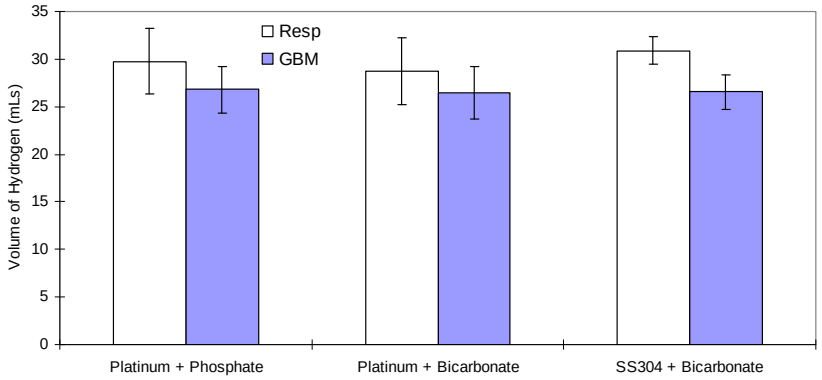


Figure 4.1: Hydrogen gas production per cycle per setup, using the gas respirometer method and the GBM (n=6)

Hydrogen production per cycle was the highest in SS304 and bicarbonate buffer using the respirometer method. For the GBM all three setups were the same, with the greatest difference between the three setups gas production being 0.4 %.

**4.5 Maximum Hydrogen Production Rate**

Maximum hydrogen production rates using the respirometer method were 2.63 ± 0.62 $m^3$ $H_2$-$m^{-3}d^{-1}$ using a platinum cathode with a phosphate buffer, 2.06 ± 0.44 $m^3$ $H_2$-$m^{-3}d^{-1}$ using a platinum cathode with bicarbonate buffer and 1.40 ± 0.13 $m^3$ $H_2$-$m^{-3}d^{-1}$ using SS304 #60 mesh cathode with bicarbonate buffer (Figure 4.2). Maximum hydrogen production rate using the GBM was lower at 1.67 ± 0.37 $m^3$ $H_2$-$m^{-3}d^{-1}$ using a platinum cathode with a phosphate buffer, 1.20 ± 0.25 $m^3$ $H_2$-$m^{-3}d^{-1}$ using a platinum cathode and bicarbonate buffer, and 1.11 ± 0.27 $m^3$ $H_2$-$m^{-3}d^{-1}$

using a SS304 #60 mesh cathode with bicarbonate buffer (Figure 4.2). On another set of batch experiments using the GBM, maximum hydrogen production was 2.10 ± 0.30 $m^3$ $H_2$-$m^{-3}d^{-1}$ using a platinum cathode with phosphate buffer, 1.38 ± 0.41 $m^3$ $H_2$-$m^{-3}d^{-1}$ using a platinum cathode with a bicarbonate buffer, and 1.33 ± 0.28 $m^3$ $H_2$-$m^{-3}d^{-1}$ using a SS304 #60 mesh cathode with bicarbonate buffer (Figure 4.2). Complete batch cycle time was 16.7 ± 4.2 hrs for a platinum cathode with phosphate buffer, 24.7 ± 5.4 hrs for a platinum cathode with bicarbonate buffer, and 26.6 ± 4.6 hrs for a SS304 cathode with bicarbonate buffer (Figure 4.2).

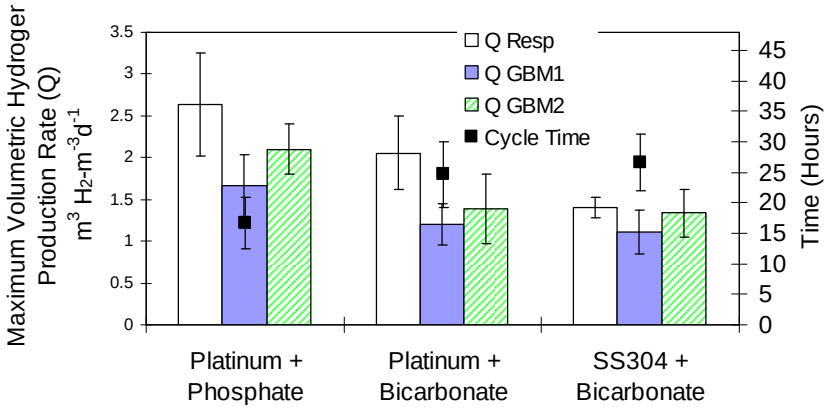


Figure 4.2 Average cycle time and maximum hydrogen production rates per setup, averaged from each cycle, using the respirometer method and GBM (n=6)

Maximum volumetric hydrogen production rate was observed to be highest across all three sets of experiments in the platinum and phosphate buffered system. Platinum and bicarbonate buffer had the second highest gas generation rates, while the lowest rates were obtained for the SS304 and bicarbonate buffered system. Reproducibility between the three sets of experiments: respirometer, GBM 1 and GBM 2 runs was low (Figure 4.2). The standard deviations of the systems were ± 0.35 $m^3$ $H_2$-$m^{-3}d^{-1}$.

**4.6 Coulombic Efficiencies**

Coulombic efficiency (CE) is calculated as the number of electrons collected in the system, compared to total electrons available by the substrate (Equation 3.12). The values should be similar regardless of measurement device, assuming similar substrate removal, and cycle time. CE using the respirometer setup was 80.3 ± 2.5 %, 94.1 ± 5.8 %, 87.1 ± 5.3 % using platinum with phosphate, platinum with bicarbonate, and SS304 #60 mesh with bicarbonate, respectively (Figure 4.3). CE using the GBM was 88.0 ± 11.1 %, 91.2 ± 6.3 %, and 71.8 ± 6.9 % using platinum with phosphate, platinum with bicarbonate, and SS304 #60 mesh with bicarbonate, respectively (Figure 4.3). Coulombic efficiency was highest in the platinum and bicarbonate buffered system.

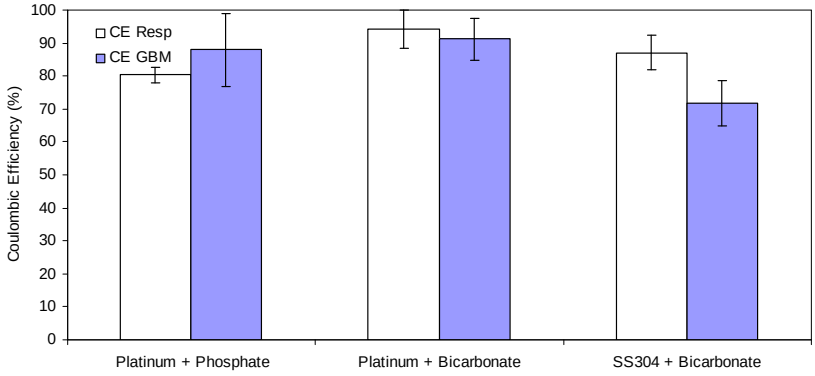


Figure 4.3: Coulombic efficiency for each setup, from the voltage data for the respirometer method and for the GBM (n=6)

**4.7 Energy Recoveries**

Electrical energy efficiency ($\eta_E$) is based on the electricity added to the system and can be over 100 %. Electrical energy efficiency was higher using the respirometer method compared to the GBM for tests with platinum and phosphate or bicarbonate. In the SS304 and bicarbonate

system the electrical energy efficiencies were close at 154.9 ± 7.5 % for the respirometer method and 159.8 ± 17.2 % for the GM (Figure 4.4).

Overall energy efficiency ($\eta_{E+S}$) was slightly higher using the respirometer method and ranged from 59.1 ± 5.6 % to 68.3 ± 7.6 % across all configurations and testing techniques (Figure 4.4).

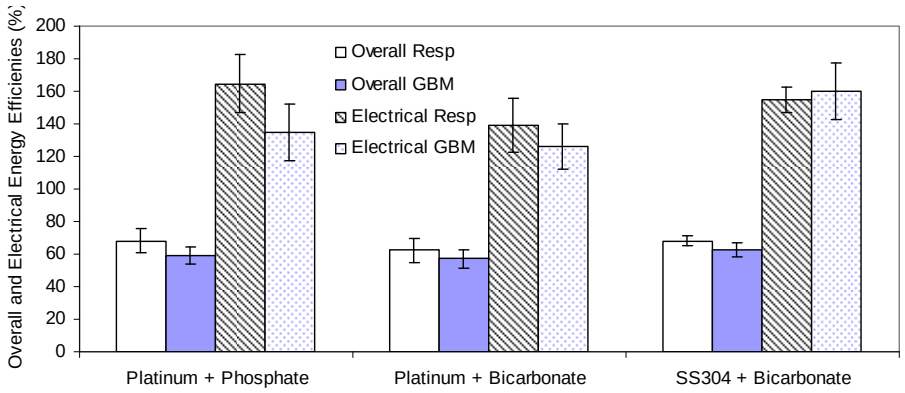


Figure 4.4 Electrical and overall energy efficiencies for the three setups using the respirometer method and the GBM (n=6)

### 4.8 SS304 Cathode with Bicarbonate Buffer at Varied Voltages

Hydrogen production increased with increased voltage from 2.1 ± 0.9 mLs$H_2$ at 0.5 V, to 24.2 ± 5.3 mL $H_2$ at 0.7 V, to 30.9 ± 1.4 mL $H_2$ at 0.9V (Figure 4.5). There was more methane produced at 0.5 V than with higher voltages (Figure 4.5). Methane production was 1.5 ± 0.4 mL $CH_4$ per cycle or 33 % of the total gas production at this applied voltage. Maximum hydrogen production rate also increased with applied voltage, going from 0.06 ± 0.06 $H_2$-$m^{-3}d^{-1}$ at 0.5 V, to 0.81 ± 0.11 $H_2$-$m^{-3}d^{-1}$ at 0.7 V, to 1.40 ± 0.13 $m^3$ $H_2$-$m^{-3}d^{-1}$ at 0.9 V (Figure 4.5).

**Comment [J1]:** You state in the text every data in the figure – redundant.

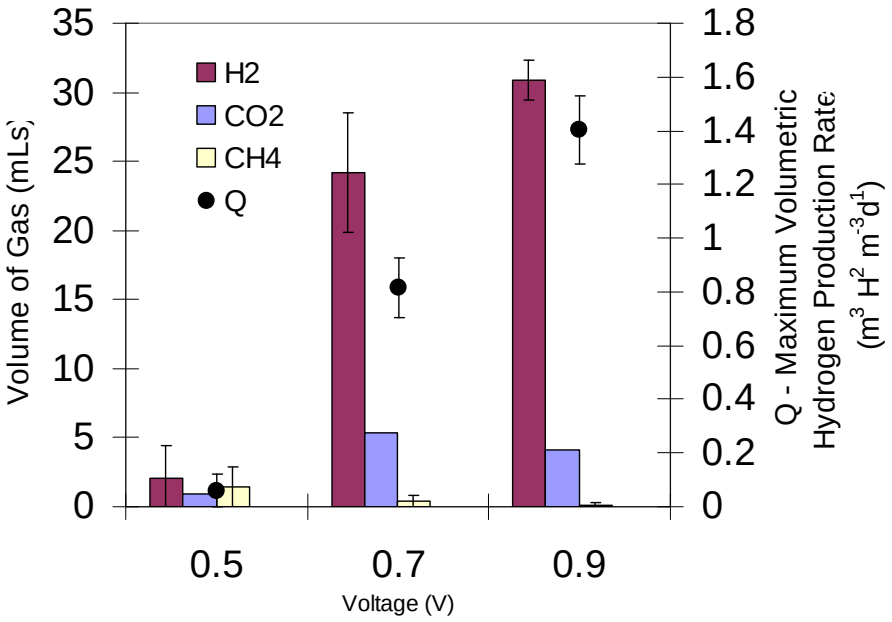


Figure 4.5 Hydrogen, carbon dioxide, methane productions per cycle and maximum hydrogen production rates at varying applied voltages using a stainless steel 304 mesh cathode with bicarbonate buffer (for 0.5 V experiments n=4, for 0.7 V and 0.9 V n=5)

Coulombic efficiency increased dramatically when the voltage was increased from 0.5 V to 0.7 V, but it remained relatively constant from 0.7 V to 0.9 V (Figure 4.6). Electrical energy efficiencies were similar at 0.7 V (158.6 ± 31.7 %) and 0.9 V (154.9 ± 7.5 %) (Figure 4.6). Electrical and overall energy efficiencies were low at 0.5 V, with $\eta_E$ = 34.9 ± 34.0 % and $\eta_{E+S}$ = 6.4 ± 5.9 % (Figure 4.6). Overall energy efficiency increased slightly from $\eta_{E+S}$ = 59.5 ± 4.5 % at 0.7 V to $\eta_{E+S}$ = 68.2 ± 2.9 % at 0.9 V (Figure 4.6).

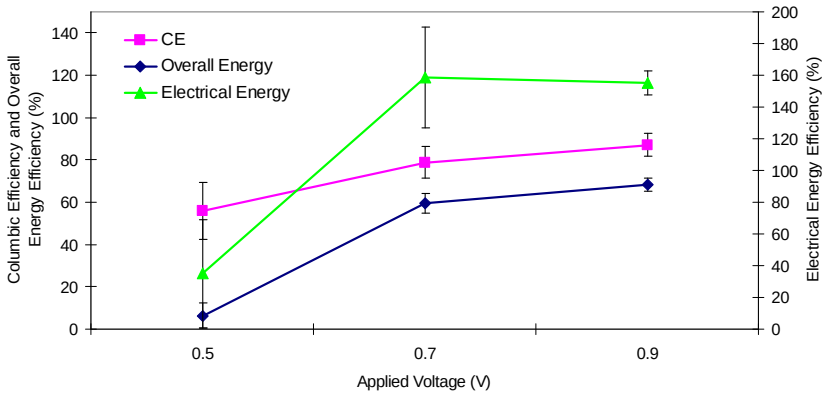


Figure 4.6 Coulombic efficiency, electrical energy efficiency and overall energy efficiency at varied voltages in a SS304 #60 mesh cathode and bicarbonate buffered system (for 0.5 V experiments n=4, for 0.7 V and 0.9 V n=5)

# Chapter 5

## Discussion:

### 5.1 Gas Bag Method

Tests using the GBM had errors of less than 6% based measurements with known conditions (Table 4.1). Possible sources of error the GBM include instrumental error, errors in GC standards, the injection volumes, and standard curves. The syringe used for additions of internal standard gas, for example, was only accurate to ± 0.2 mL. Based on these results, the GBM appears to be an acceptable method for quantifying gas production in MECs.

$H_2$ production values were higher in MEC tests using the respirometer method than with the GBM (Figure 4.1). This leads to higher maximum hydrogen production rates, electrical energy efficiency, and overall energy efficiency values (Equations 3.14, 3.18, 3.19 and Figures 4.6, 4.8). The differences between hydrogen estimates for the respirometer method and using the GBM are not completely understood and could use more investigation and discussion.

There are two potential sources of error. The respirometer counts all gas bubbles produced and we assume that all gas produced is $H_2$, $CO_2$, or $CH_4$ (Equation 3.1). This assumption could possibly lead us to overestimate the biogas production due to water vapor in the pore spaces. There is a headspace above the reactor of 10-12 mL, a headspace in the respirometer of ~15-18 mL, open space in the tubing, and a gas bag with 30-40 mL of volume (Figure 3.3). These headspaces are likely saturated with water vapor, saturated vapor pressure at 30 °C is 0.0418 atm or 4.18 %. Using the ideal gas law at 30 °C ($PV=nRT$) these open volumes could produce an approximate volume of water vapor at saturation of ~2.5 mL. Using nitrogen, oxygen and water vapor free values (Equation 3.1) the hydrogen percentages in the gas bag are in the 80-90 % range. This could translate to a hydrogen increase of 2 mL or more due to the additional

water pressure. In the GBM there are no assumptions made that all gasses are biogases. The final percentage of each gas is not adjusted because all gasses are in the headspace or the gas bag. In the respirometer method some biogases are left in the respirometer headspace and some are possibly dissolved in the respirometer oil.

The amount of tubing and fittings were minimized in the GBM compared to the respirometer method (Figure 3.4), reducing the possibility of gas losses due to a slightly higher pressure in the MEC compared to atmospheric. When the gas volume of a gas bag attached to a respirometer was calculated using the GBM, an average of 4.4 mLs of gas accounted for in the respirometer system was not shown in the GBM (Table 4.2). This loss does not appear to have just been hydrogen, as hydrogen percentages were the same using both the respirometer method and the GBM (Table 4.2). It is possible that the respirometer counted the gas produced, but some gas slowly diffused and left the system. This might cause biogas to be correctly accounted for in the respirometer system but not be present in the gas bag system.

It was difficult to measure low volumes of gases using a respirometer especially volumes less than 10 mL. This is because sufficient gas must be produced to generate enough pressure to produce bubbles in the barrier solution and a minimum amount must be made in order to become detectable within the large volume of open space in the respirometer system (Figure 3.3). To get an accurate characterization of the gas at least one open air volume of the respirometer and tubes should be produced, with accuracy increasing with the volume of gas produced. With low biogas production, most of the gas in the gas bag will be nitrogen, but as gas production increases the percentage of biogas will increase to a level that can be more accurately measured. With the GBM there is no barrier solution, so little pressure is required to pass biogas into the gas bag. The only nitrogen in the system is in the headspace of the reactor and the residual nitrogen left over in the gas bag. This means that even with low gas production the amount of gas produced can be accurately determined.

**5.2 Conductivity and pH**

Solution conductivity and pH did not change appreciably during the batch cycles (Table 4.3), even though the carbon dioxide produced in the bicarbonate systems was higher than that of the phosphate system (Appendix C). This increase in carbon dioxide was likely due to release from the bicarbonate buffer. Another possibility is that the excess bicarbonate in solution caused carbon dioxide produced by reaction 2.3 to have a higher tendency to evolve rather then stay in solution. Even if there was bicarbonate leaving the system by $CO_2$ evolution, the loss did not cause conductivity to decrease over a batch cycle (Table 4.3). In the phosphate buffer the carbon dioxide produced may be more likely to stay in solution. This addition of $CO_2$ did not appreciably increase the conductivity of the phosphate solution (Table 4.3).

**5.3 MEC Performance by Setup**

Hydrogen production per cycle was comparable for the three different cell setups (Figure 4.1). Maximum volumetric hydrogen production rate (Q) was appreciably lower using the bicarbonate buffer than with a phosphate buffer, and the platinum cathode versus the SS304 cathode, in all three experiments (1 respirometer, 2 GBMs) (Figure 4.2). The maximum volumetric hydrogen production rate is partially based on volumetric current densities (Equation 3.14). Higher maximum currents in the platinum cathode MECs, compared to those using SS 304, increased Qs while not increasing the total hydrogen produced per cycle. Lower current densities led to increased batch completion times (Figure 4.2). Maximum volumetric hydrogen production rates for platinum and phosphate buffer at 0.85 V reported in the literature have reached as high as 3.35 $m^3$ $H_2$-$m^{-3}d^{-1}$ with the highest at any voltage of 6.32 $m^3$ $H_2$-$m^{-3}d^{-1}$ at 1.1V [40]. In this study, Q reached 3.36 $m^3$ $H_2$-$m^{-3}d^{-1}$, but the average rate was much lower. This variable Q value suggests that either the anodic biofilm or the cathode were less stable in these experiments. The maximum reported volumetric hydrogen production rates for a high surface area SS304 brush in a phosphate buffer at 0.6 V was 1.7 $m^3$ $H_2$-$m^{-3}d^{-1}$ [20]. This value is approximately twice as high as found in this study for SS304 mesh cathodes and a bicarbonate buffer at 0.7 V (Figure 4.5). This

difference is attributed to the higher current densities in the SS304 brush setup due to the increased surface area.

The increased cycle time in the bicarbonate systems can be attributed to overpotentials associated with the bicarbonate buffer and the SS304 mesh (Figure 4.2). Buffers have been reported to perform comparably when the conductivity is similar [43], but only using buffers with a pH of ~7. The bicarbonate and phosphate buffers have similar conductivities, but the initial pH of the bicarbonate buffer was 8.9 ± 0.2 while the initial pH of the phosphate buffer was 7.1 ± 0.0 (Table 4.3). That is nearly a 100 fold decrease in hydrogen ions available in the bicarbonate buffer. It has been observed that there is 60 mV loss due to overpotential per pH unit [31]. This loss of potential will cause lower current densities and therefore slower substrate utilization, which increases batch time and decreases maximum hydrogen production values (Figure 4.2).

An MEC with a stainless steel 304 cathode and bicarbonate buffer produced the same hydrogen volume per cycle as an MEC with a platinum cathode and bicarbonate buffer (Figure 4.1). Maximum hydrogen production values were lower in an MEC using a SS304 cathode than a Pt cathode (Figure 4.2). Selembo et al. found that the performance of a SS 304 plate cathode was nearly identical to that of a platinum plate cathode in a MEC [25]. However, Selembo et al. later found that at a fixed current density SS304 particles had an overpotential of -0.813 V compared to an overpotential of -0.500 V with platinum [26]. This overpotential results in lower current densities at the same applied voltage, which leads to slower utilization of substrate.

Coulombic efficiencies (CE) ranged from 71.8 ± 6.9 % to 94.1 ± 5.8 % across all setups (Figure 4.3), assuming complete acetate removal. This is a reasonable assumption as acetate removal efficiencies are reported at 89.2 ± 0.8 % [17], 91 ± 5 % [49] and as high as 98 ± 0 % [17] in similar setups, however complete removal of acetate based on COD measurements is not always reported. The assumption of 100 % removal efficiency of acetate could decrease the calculated coulombic efficiency values because missing coulombs could leave the system as acetate. The coulombic efficiency was not consistent across gas measurement methods

(respirometer and GBM) for the stainless steel 304 cathode, as the CE increased from 71.8 ± 6.9 to 87.1 ± 5.3 % when switching from the GBM to the respirometer method. CE could have changed with a shift in a microbial community between test cycles or could have been due to improper cycle termination times by uncertain batch finish times. Batch times were different in each setup and the lower current densities in reactors not using platinum cathode could have led to early disconnection.

Electrical energy efficiencies were higher using the platinum cathode and a phosphate buffer compared to the bicarbonate buffer (Figure 4.4). Electrical energy efficiency was expected to drop from the platinum cathode and bicarbonate buffer to the SS304 cathode and bicarbonate buffer due to SS304 being a less efficient catalyst than platinum, however the electrical energy increased (Figure 4.4). $W_E$ was lower in the SS304 cathode system, while hydrogen production was similar to the platinum cathode system. This caused electrical energy efficiency to be higher in the SS304 system.

Overall energy efficiencies were similar across setups. The drop in energy efficiency from the respirometer method to the GBM can be explained by the higher reported production of $H_2$ using the respirometer system. The energy efficiencies reported in the literature for a phosphate buffer and a platinum cathode at an applied voltage of 0.8 V are all higher than obtained in this study with 74.9 ± 1.4 % for overall energy efficiency and 193.8 ± 1.8 % for electrical energy efficiency [17]. The maximum reported electrical energy efficiencies were at 0.3 V applied, while the maximum reported overall energy efficiencies were at 0.4 V due to an increase of cathodic recoveries [17]. This suggests that there should be some efficiency increase going from 0.9 V to 0.8 V, as the applied voltage moves towards the maximum of 0.4 V. Overall and electrical energy efficiencies for a stainless steel brush with a high surface area at 0.6 V applied with a phosphate buffer have been reported at 78 ± 5 % and 221 ± 8 % respectively [20], which is higher then that reported in this study with bicarbonate buffer at voltages of 0.5 V, 0.7 V,

and 0.9V (Figure 4.6). The surface area of the cathode appears to have decreased the MEC's efficiencies. Call et al. found that current density of a stainless steel brush decreased from 91 $A/m^3$ to 78 $A/m^3$ when the surface area of the cathode was decreased by 75 % [20]. This stainless steel brush cathode had a specific surface area of 810 $m^2/m^3$ or ~12 times of the SS304 mesh #60 cathode measured by Zhang (2010) [20].

**5.4 SS 304 and Bicarbonate Buffer Performance with Varied Voltages**

An applied voltage of 0.5 V appeared to approach the lower limit for hydrogen production possible using a bicarbonate buffer and stainless steel electrode. The Q, CE, $\eta_E$, and $\eta_{E+S}$ were all much lower with a 0.5 V applied as compared to at 0.7 V and 0.9 V applied (Figure 4.5 and Figure 4.6). The SS304 cathode and bicarbonate buffered system had larger overpotentials, cathodic efficiencies and solution pHs than the Pt cathode and phosphate buffer based. These overpotentials, combined with the small applied voltage of 0.5 V, caused increased cycle time, considerable losses of hydrogen to methane, and a significant drop off of hydrogen production when compared to the 0.7 V system (Figure 4.5). Overpotentials due to solution pH and cathodic efficiencies can be attributed to the system approaching the minimum voltage needed to produce hydrogen. CE, $\eta_E$, and $\eta_{E+S}$ remained essentially constant for both 0.7 V and 0.9 V applied voltages (Figure 4.6). The lower applied voltages produced lower current densities and increased the uncertainty of end point of the run, especially with 0.5 V and 0.7 V applied voltages. This difficulty could have led to the premature ending of some runs which may have caused decreases in CEs and hydrogen production.

# Chapter 6

## Conclusions

SS304 mesh #60 cathodes and bicarbonate buffer have shown potential to be technically feasible, and thus a more economical approach for upscaling MEC reactors, based on energy efficiencies compared to platinum cathodes and a phosphate buffer. The applied voltage should be kept > 0.5 V in order to keep energy efficiency high and cycle times short, which will minimize methanogenisis. Gas volumes reported with the GBM were shown to be accurate to ~5 %. The results showed that:

1. MECs with SS304 mesh #60 cathodes and a bicarbonate buffer performed similarly to reactors with platinum cathodes and a phosphate buffer in terms of hydrogen production per cycle, electrical energy efficiency and overall energy efficiency.
2. MECs with SS304 cathodes and a bicarbonate buffer operated at voltages above 0.5 V achieve high electrical energy efficiencies and overall electrical energy efficiencies.
3. The GBM is a reproducible and accurate method for quantifying the gas production of MECs.

# Chapter 7

## Future Work

There are some items which could be studied more to make this work more complete:

1. MECs with bicarbonate buffer and SS304 #60 mesh cathode could be run for more cycles to try and understand the time it takes for methanogen populations to affect hydrogen production. SS304 and bicarbonate would appear to be a better environment for methanogens because of the longer cycle times and availability of bicarbonate for growth, though high methane production was not observed in this study.
2. The difference between the values of gas produced between the GBM and the respirometer method should be investigated further to better understand the reasons for higher estimated hydrogen production with the respirometer
3. Preacclimation of the microbial community to a bicarbonate buffer before switching from MFC to MEC would be of interest to see if the anode community would respond more efficiently, and consistently to this buffer.
4. The applied voltage could be systematically increased on the SS304 cathode and bicarbonate buffered system to find the minimum applied voltage where hydrogen is produced in a system and the highest voltage where methane is still produced.

## Appendix A

## GBM Example

Example GC output of a gas bag with a $H_2$ and $N_2$ mix using a gastight syringe (250 µL, Hamilton Samplelock Syringe):

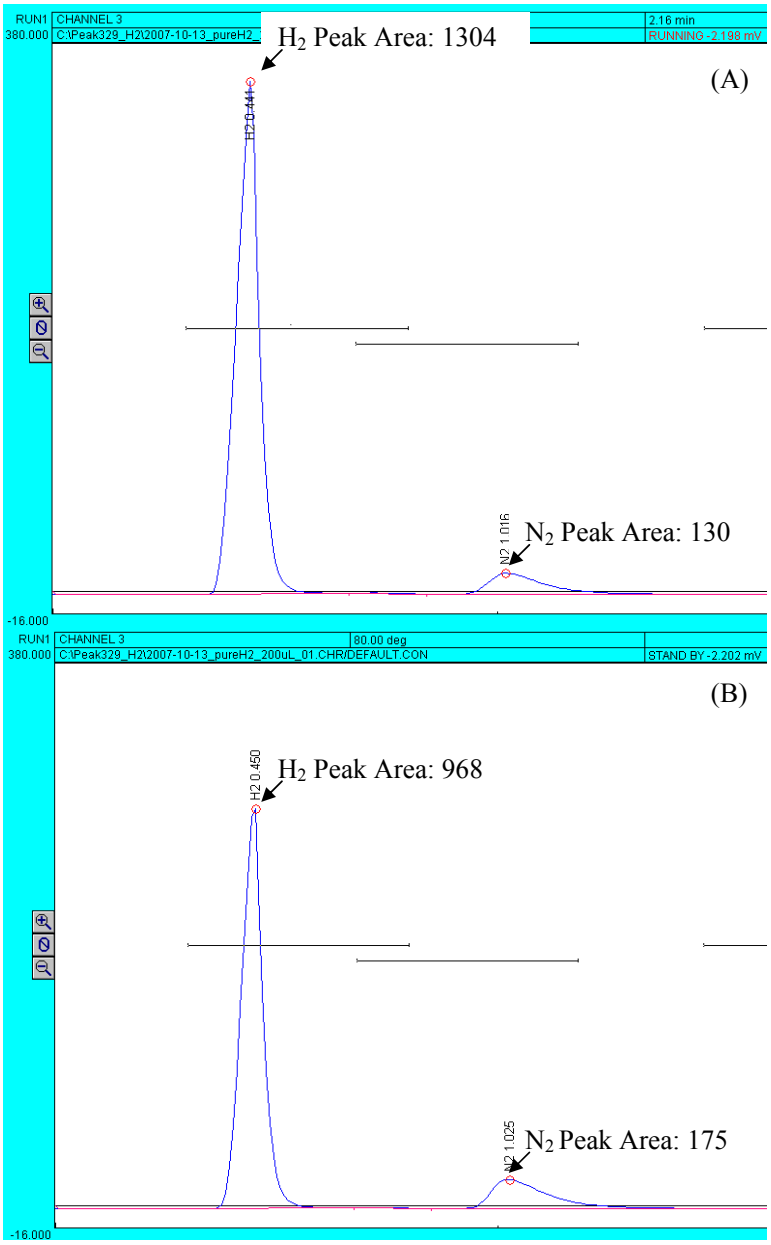

Figure A.1: GC output of a gas bag containing $H_2$ and $N_2$ before the addition of a 10mL $N_2$ tracer (A) and after the tracer addition (B)

To find the gas volumes of $H_2$ and $N_2$ in the gas bag using the GBM equations 3.4 through 3.9 are used.

Assumptions: 3 GC injections were made before tracer addition.

The average peak areas are $H_2$: 1304 and $N_2$: 130

3 GC injections after tracer addition average $H_2$: 968 and $N_2$: 175

GC standard curve for $H_2$: $Mole\ Fraction\ Hydrogen = H_2\ Peak\ Area \times 0.000383$

GC standard curve for $N_2$: $Mole\ Fraction\ Nitrogen = N_2\ Peak\ Area \times 0.00385$

Using equation 3.4 we can find the volume lost due to GC injections:

$V_L = 3 * 0.25\ mL = 0.75\ mL\ lost$

Using the standards given we can find the original mole percentages of the gases:

$$x_{T,b,i} = 130 \times 0.00385 = 0.5 \frac{mol\ N_2}{mol\ total}$$

Using equation 3.5 we can find the volume of the tracer gas in the bag before tracer addition:

$$x_{H2,b,i} = 1304 \times 0.000383 = 0.5 \frac{mol\ H_2}{mol\ total}$$

then the initial volume of tracer in the gas bag:

$$V_{T,b,i} = 0.5 \frac{mol\ N_2}{mol\ total} V_{b,i}$$

Using the standards we can find the final mole percentage of the tracer gas:

$$x_{T,b,f} = 175 \times 0.00385 = 0.67 \frac{mol\ N_2}{mol\ total}$$

Plugging equation 3.6 into equation 3.7 we can find the initial total volume of the gas bag:

$$V_{b,i} = \frac{-10\ mLs\ N_2\ added + 0.75\ mL\ lost \times 0.5\ \frac{mol\ N_2}{mol\ total} + 10\ mLs\ N_2\ added \times 0.67\ \frac{mol\ N_2}{mol\ total} - 0.75\ mL\ lost \times 0.67\ \frac{mol\ N_2}{mol\ total}}{0.5\ \frac{mol\ N_2}{mol\ total} - 0.67\ \frac{mol\ N_2}{mol\ total}}$$

$$V_{b,i} = 20\ mL$$

Then using equation 3.8 (with the $V_h=0$ because we're only looking at the gas bag) the volume of $H_2$ can be determined:

$$V_{H2} = 0 + 0.5\frac{mol\ H_2}{mol\ total} \times 20\ mL = 10\ mL\ H_2$$

And the volume of $N_2$ can be determined using equation 3.8 and substituting hydrogen percentages with nitrogen percentages:

$$V_{N2} = 0 + 0.5\frac{mol\ N_2}{mol\ total} \times 20\ mL = 10\ mL\ N_2$$

## Appendix B

### Typical MEC Results

Example results from a MEC with a platinum cathode and a phosphate buffer:

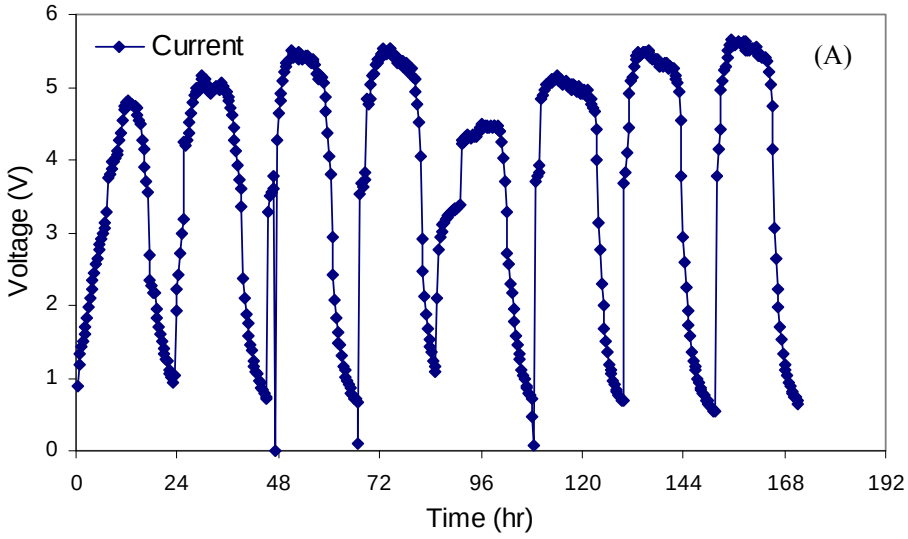


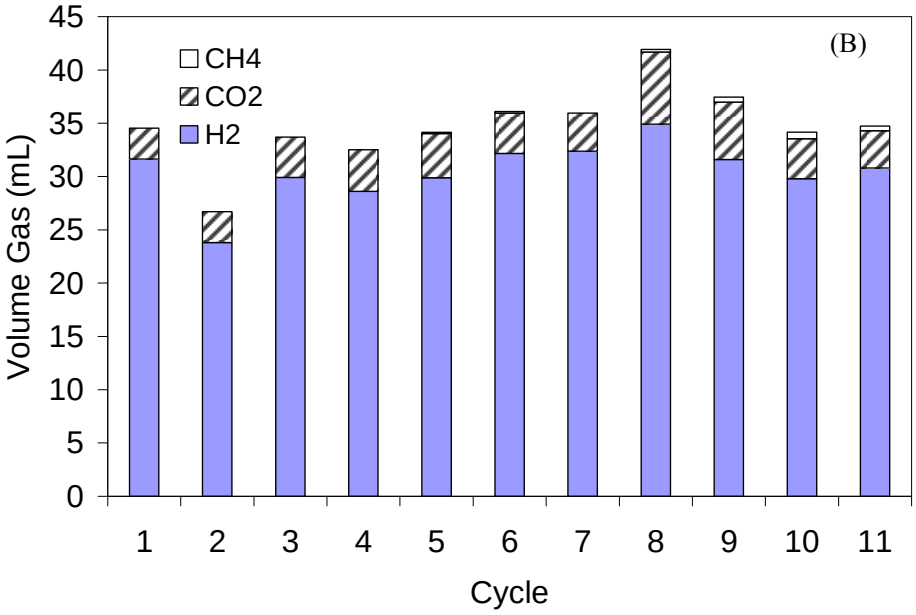

Figure B.1: Current output (A) and biogas production per cycle (B) for a MEC with a phosphate buffer and a platinum cathode

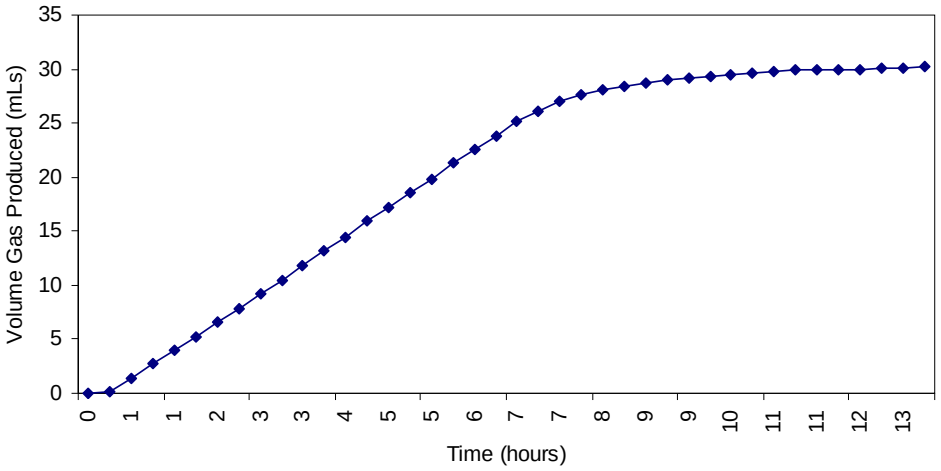


Figure B.2: Example respirometer data for a MEC with a phosphate buffer and a platinum cathode

## Appendix C

### Carbon Dioxide Production

Carbon dioxide results in all three set ups using both the GBM and the respirometer method.

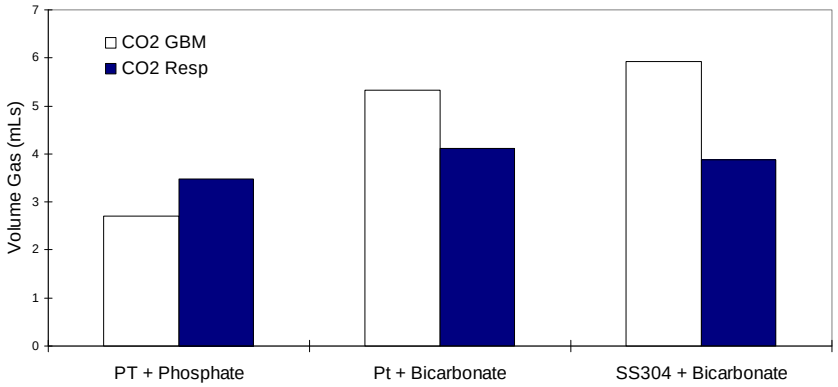


Figure C.1: Carbon dioxide found in a MEC with a platinum cathode and phosphate buffer, platinum cathode with a bicarbonate buffer and SS304 with a bicarbonate buffer using both the respirometer method and the GBM (n=7)

## Appendix D

### Tracer Gas Selection Process

Here are the steps leading to $N_2$ being chosen as the internal standard gas for the GBM.

When the GBM was first being conceptualized the thought was that a separate gas not produced or present already in a MEC environment would be required. With that we tried to find gases which had different thermal conductivities then our carrier gases, Ar and He, as well as good separation from other gases using our 6 foot molecular sieve packed 5A column and 6 foot porapak Q column. We tried several gases, however none matched the previous two constraints while still being low cost and non hazardous. We then tried switching the carrier gases of the GCs in an attempt to find a combination which would allow us to continue testing for $H_2$, $CO_2$, and $CH_4$ while also allowing us to get a separate and distinguishable peak for a standard gas.

Using Table D.1 we tried several combinations but ended up on switching the carrier gas of the molsieve column from Ar to $N_2$. This allowed us to detect $H_2$, Ar, and $CH_4$ on the molsieve column while still being able to detect and measure $CO_2$ on the porapak column. Ar could then be used as the internal standard gas. There were two issues with this set up. First the Ar conductivity is less than the $N_2$ carrier while all the other gasses of concern are greater then the carrier (Table D.1). This meant the difference in conductivity was negative, which was a problem for the software we use because it can only measures positive peaks. This could be fixed by manually switching the polarity of the output during the cycle or by running the sample twice, once at positive polarity and once at negative polarity. Manually switching the polarity was difficult to repeat accurately, while doing two runs doubled the amount of time needed for GC injections. Secondly the separation of the peaks of Ar and $H_2$ were not great. This compounded with the first problem because the $H_2$ peak would need to finish eluting entirely before a polarity switch in order to record the correct value for $H_2$. We solved this by increasing the length of the column,

first to 9 feet, but then to 12 feet. This increased the GC cycle times, while also increased the time separating the $H_2$ and Ar peaks.

This configuration allowed us to inject a known amount of argon and estimate the area of the peak, which could then be used to find total volume. However, it increased the time for injections as well as added human error in manual integration and shifting the polarity. Trying to solve these issues we realized that it wasn't necessary that the gas be an original gas to the system. If we used a gas already in the system we could figure out the volume of the gas bag by estimating the mole percentages before and after the addition of the tracer (Equations 3.4 to 3.9). We shifted back to the original 6 foot columns with Ar and He as the carrier gases and selected $N_2$ as the internal standard due to its large and repeatable peak areas as well as its' low cost.

Table D.1 Thermal conductivities of select gases at 25 °C (298 K) [51]

| Gas | Thermal Conductivity at 298 K ($Wm^{-1}K^{-1}$) |
|---|---|
| Ar | 0.016 |
| $N_2$ | 0.024 |
| $O_2$ | 0.024 |
| $H_2$ | 0.168 |
| $CH_4$ | 0.030 |
| $CO_2$ | 0.0146 |
| He | 0.142 |
| $H_20$ (at 398 K) | 0.016 |

**Literature Cited**


1. *Monthly Energy Review*. 2009, U.S. Energy Information Administration: Washington, DC.
2. Newell, R., *Annual Energy Outlook 2010 Reference Case*. 2009, US Energy Information Administration: Washington, DC. p. 6-21.
3. *Oil Market Report*. 2009, International Energy Agency. p. 6.
4. *Oil Market Report*. 2006, International Energy Agency. p. 4.
5. *Oil Market Report*. 2005, International Energy Agency. p. 4.
6. Robert L. Hirsch, R.B., Robert Wendling, *Peaking of World Oil Production: Impacts, Mitigation, & Risk Management*. 2005. p. 5.
7. *Drivers of the Energy Scene*. 2003, World Energy Council.
8. Laherrere, J., in *Seminar Center of Energy Conversion Zurich May 7 2003*. 2003: Zurich.
9. *Emissions of Greenhouse Gases in the United States in 2008*. 2009, U.S. Energy Information Administration: Washington, DC. p. 2.
10. *The Impact of Increased Use of Hydrogen on Petroleum Consumption and Carbon Dioxide Emissions*. 2008, U.S. Energy Information Administration.
11. Ni, M., et al., *An overview of hydrogen production from biomass.* Fuel Processing Technology, 2006. **87**(5): p. 461-472.
12. Takahashi, J.Y.a.P., *Biophotolysis-based Hydrogen Production by Cyanobacteria and Green Microalgae.* Communicating Current Research and Educational Topics and Trends in Applied Microbiology, 2007.
13. Lee, H.-S., W.F.J. Vermaas, and B.E. Rittmann, *Biological hydrogen production: prospectives and challenges.* Trends in Biotechnology. **In Press, Corrected Proof**.
14. Hussy, I., et al., *Continuous fermentative hydrogen production from a wheat starch co-product by mixed microflora.* Biotechnology and Bioengineering, 2003. **84**(6): p. 619-626.
15. Fang, C.L.a.H.H.P., *Fermentative Hydrogen Production From Wastewater and Solid Wastes by Mixed Cultures.* Critical Reviews in Environmental Science and Technolgy, 2007(37): p. 1-39.
16. Liu, H., S. Grot, and B.E. Logan, *Electrochemically assisted microbial production of hydrogen from acetate.* Environmental Science & Technology, 2005. **39**(11): p. 4317-4320.
17. Call, D. and B.E. Logan, *Hydrogen production in a single chamber microbial electrolysis cell (MEC) lacking a membrane.* Environmental Science & Technology, 2008. **42**(9): p. 3401-3406.
18. Logan, B.E., *Microbial fuel cells*. 2008, Hoboken, NJ: John Wiley & Sons, Inc. 300.
19. Ivy, J., *Summary of Electrolytic Hydrogen Production*. 2004, NREL.
20. Call, D., M.D. Merrill, and B.E. Logan, *High surface area stainless steel brushes as cathodes in microbial electrolysis cells (MECs).* Environmental Science & Technology, 2009. **43**(6): p. 2179-2183.

21. Lalaurette, E., et al., *Hydrogen production from cellulose in a two-stage process combining fermentation and electrohydrogenesis.* International Journal of Hydrogen Energy, 2009: p. in press.
22. Selembo, P.A., et al., *High hydrogen production from glycerol or glucose by electrohydrogenesis using microbial electrolysis cells.* International Journal of Hydrogen Energy, 2009. **34**(13): p. 5373-5381.
23. Rozendal, R.A., et al., *Towards practical implementation of bioelectrochemical wastewater treatment.* Trends in Biotechnology, 2008. **26**(8): p. 450-459.
24. *Platinum Today: Price Charts*. 2010 [cited 2010 January 27th, 2010]; Available from: http://www.platinum.matthey.com/pgm-prices/price-charts/.
25. Selembo, P.A., M.D. Merrill, and B.E. Logan, *The use of stainless steel and nickel alloys as low-cost cathodes in microbial electrolysis cells.* Journal of Power Sources, 2009. **190**(2): p. 271-278.
26. Selembo, P.A., M.D. Merrill, and B.E. Logan, *Hydrogen production with nickel powder cathode catalysts in microbial electrolysis cells.* International Journal of Hydrogen Energy. **35**(2): p. 428-437.
27. Sun, M., et al., *An MEC-MFC coupled system for biohydrogen production from acetate.* Environmental Science & Technology, 2008. **42**(21): p. 8095–8100.
28. Correll, D.L., *The Role of Phosphorus in the Eutrophication of Receiving Waters: A Review.* J. Environ. Qual., 1998. **27**: p. 261-266.
29. Cordell, D., J.-O. Drangert, and S. White, *The story of phosphorus: Global food security and food for thought.* Global Environmental Change, 2009. **19**(2): p. 292-305.
30. Fan, Y., H. Hu, and H. Liu, *Sustainable power generation in microbial fuel cells using bicarbonate buffer and proton transfer mechanisms.* Environmental Science & Technology, 2007. **41**(23): p. 8154-8158.
31. Merrill, M.D. and B.E. Logan, *Electrolyte effects on hydrogen evolution and solution resistance in microbial electrolysis cells.* Journal of Power Sources, 2009. **191**(2): p. 203-208.
32. Walker, M., et al., *Potential errors in the quantitative evaluation of biogas production in anaerobic digestion processes.* Bioresource Technology, 2009. **100**(24): p. 6339-6346.
33. Selembo, P. *Stainless Steel and Nickel Cathodes in Microbial Electrolysis Cells*. in *AEESP*. 2009.
34. Logan, B.E., et al., *Microbial electrolysis cells for high yield hydrogen gas production from organic matter.* Environmental Science & Technology, 2008. **42**(23): p. 8630-8640.
35. Ditzig, J., H. Liu, and B.E. Logan, *Production of hydrogen from domestic wastewater using a bioelectrochemically assisted microbial reactor (BEAMR).* International Journal of Hydrogen Energy, 2007. **32**(13): p. 2296-2304.
36. Rozendal, R.A., et al., *Principle and perspectives of hydrogen production through biocatalyzed electrolysis.* International Journal of Hydrogen Energy, 2006. **31**(12): p. 1632-1640.
37. Cheng, S. and B.E. Logan, *Sustainable and efficient biohydrogen production via electrohydrogenesis.* Proceedings of the National Academy of Science, 2007. **104**(47): p. 18871-18873.

38. Rozendal, R., et al., *Performance of single chamber biocatalyzed electrolysis with different types of ion exchange membranes.* Water Research, 2007. **41**: p. 1984-1994.
39. Hu, H., Y. Fan, and H. Liu, *Hydrogen production using single-chamber membrane-free microbial electrolysis cells.* Water Research, 2008. **42**(15): p. 4172-4178
40. Tartakovsky, B., et al., *High rate membrane-less microbial electrolysis cell for continuous hydrogen production.* International Journal of Hydrogen Energy, 2008: p. doi:10.1016/j.ijhydene.2008.11.003.
41. Chae, K.J., et al., *Biohydrogen productin via biocatalyzed electrolysis in acetate-fed bioelectrochemical cells and microbial community analysis.* International Journal of Hydrogen Energy, 2008: p. doi:10.1016/j.ijhydene.2008.05.013.
42. Rozendal, R.A., et al., *Hydrogen production with a microbial biocathode.* Environmental Science & Technology, 2008. **42**(2): p. 629-634.
43. Nam, J.-Y., et al., *Variation of power generation at different buffer types and conductivities in single chamber microbial fuel cells.* Biosensors & Bioelectronics, 2009: p. doi:10.1016/j.bios.2009.10.005.
44. Call, D.F., R.C. Wagner, and B.E. Logan, *Hydrogen production by Geobacter species and a mixed consortium in a microbial electrolysis cell.* In preparation., 2009.
45. Cesar, I.T., M. Andrew Kato, and E.R. Bruce, *Phosphate and Bicarbonate Buffers as Proton Carriers Inside the Biofilm of Anode-Respiring Bacteria in Microbial Fuel Cells.* ECS Meeting Abstracts, 2008. **801**(7): p. 239.
46. *World Stainless Steel Prices from MEPS*. 2009, MEPS.
47. Owen, W.F., et al., *Bioassay for monitoring biochemical methane potential and anaerobic toxicity.* Water Research, 1979. **13**: p. 485-493.
48. Logan, B.E., et al., *Biological hydrogen production measured in batch anaerobic respirometers.* Environmental Science & Technology, 2002. **36**(11): p. 2530-2535.
49. Lalaurette, E., *Hydrogen Production from Cellulose Fermentation End Products Using Microbial Electrolysis Cells*, in *Environmental Engineering*. 2008, Pennsylvania State University. p. 12.
50. Cheng, S. and B.E. Logan, *Ammonia treatment of carbon cloth anodes to enhance power generation of microbial fuel cells.* Electrochemistry Communications, 2007. **9**(3): p. 492-496.
51. *Thermal Conductivity of Some Common Materials*. 2005 [cited 2010 April 12]; Available from: http://www.engineeringtoolbox.com/thermal-conductivity-d_429.html.